Numerical modeling of a river site for in-stream energy converters

E. Lalander[1] and M. Leijon[1]

[1]The Swedish Center for Renewable Electric Energy Conversion,
Division of electricity,
Department of Engineering Sciences,
Uppsala University,
Box 534, SE-751 21 Uppsala, Sweden

Abstract

Current measurement in the river Dalälven, situated in Sweden, was compared with flow values. These were also used to validate a numerical simulation of the channel. The results showed the numerical program was able to assess the current speed variations, but the magnitude of the current speed was slightly lower than the measured values, a possible effect of bathymetry errors. The water level variations were not correctly assessed, which is probably due to that wind data was excluded.

The numerical program was used to evaluate how large the effects on the surrounding water level and current speed can be for a set of ten turbines distributed evenly along the channel. To investigate how the hydrography of the channel is affected by energy extraction, a set of ten turbines distributed evenly along the channel were put into the numerical model. It showed that extracting 75 kW would increase the water level at the power station (upstreams) from the level at the same place without any turbines with 5.5%, and 135 kW would lead to an 8.8% increase, assuming a constant water level at the downstream boundary. With increasing c_d-values, the velocity around the turbines increases, while it decreases at the turbine.

Keywords: numerical modeling, river, energy conversion

Nomenclature

A_e	=	Turbine area [m^2]
c_d	=	Turbine drag coefficient
c_f	=	Bottom drag coefficient
c_s	=	Smagorinsky coefficient
d	=	Still water depth [m]
F_t	=	Effective drag force by a turbine [N]
g	=	Acceleration due to gravity [m/s^2]
h	=	Total water depth [m]
l	=	Grid length scale [m]
M	=	Manning number [m$^{1/3}$/s]
η_A	=	Measured water level (deviation from mean)[m]
η_L	=	Lake water level [m]
η_M	=	Simulated water level [m]
η_{M*}	=	Simulated water level extracted at ADCP location [m]
ρ	=	Density of water [kg/m^3]
Q	=	Flow from power station [m^3/s]
S_{ij}	=	Deformation rate [m^2/s]
$\vec{\tau}_b$	=	Bottom friction [N/m^2]
$\vec{u}_M$	=	Simulated horizontal velocity[m/s]
U_A	=	Measured current speed [m/s]
U_M	=	Simulated horizontal current speed [m/s]
U_{M*}	=	Simulated current speed extracted at ADCP location [m/s]
V	=	Velocity acted on a turbine [m/s]
ν_t	=	Horizontal eddy viscosity [m^2/s]

1 Introduction

River flows are formed by atmospheric precipitation and the magnitude of the flow also varies with season. At high latitudes (>60°N), during winter, the precipitation is locked as snow, and during spring time the water is released as the atmospheric temperature increases. In unregulated river courses the flow peaks at spring time as snow melts in the mountains and is reasonably constant the rest of the year. In regulated rivers which are controlled by hydropower, the flow can be controlled by the use of dams and varies with, among other factors, electricity consumption. In these rivers, the flow can vary greatly within minutes, which can have a negative impact on downstream constructions.

In Sweden, one of the main energy sources is hydropower, and most rivers are regulated. With the aim of finding new sources for the production of electricity in Sweden, together with the fact that river exploitation by conventional hydropower is reaching a maximum, interest in other renewable energy sources has increased. Only between 2006 and 2007 the installed wind power increased by 40% [1]. Even in regulated rivers there are watercourses with high kinetic energy density as will be discussed in this paper. With this background an assessment of the kinetic energy resource in Swedish rivers is of interest.

Water in rivers flows downhill driven by potential energy. This potential energy has traditionally been converted to electricity by hydropower turbines. Less common is to extract the kinetic energy in river flows using in-stream mounted turbines, although this has gained increased attention in the past years, and various methods to do this are described in [2]. The concepts are similar to tidal energy systems, although smaller in scale, but the information can be mutually valuable for both research areas.

The extraction of kinetic energy from moving water is highly dependent on the current speed and for a resource assessment it is therefore important that the nature of the flow is accurately described. Numerical methods have been used in e.g. [3] where time series of the velocity around Portland Bill were produced, in [4] where effects of tidal energy extraction at Portland Bill was estimated and in [5] where the extractable resource in Johnston Strait was calculated using a numerical model. However, input to these models has been data from sea-charts where the tidal current speed has been calculated by tidal constituents. Data from water gauging stations have been used to validate these models, whereas real time current speed data are rarely used. To measure velocity variations in time over an entire water column, an Acoustic Doppler Current Profiler (ADCP) can be used. This was utilized in [6] to measure wave induced short time fluctuations, and in [7] to compare with a numerical model of the tidal energy resource.

The aim of this work is to compare measured data to predictions from a numerical model and to increase the understanding of the resource for in-stream current energy converters. In order to do that, the current velocity was sampled with an ADCP in a Swedish river during one month. The velocity measurements were compared with numerical simulations of the site and data of flow and water level. By including a set of 10 turbines it was possible to estimate how energy extraction could affect the surrounding water levels and velocity.

2 Site description and measurement

There are approximately 15 rivers with a flow rate of more than 100 m^3/s in Sweden. Most of these rivers are exploited by hydropower and the majority are situated in the north of Sweden, having their discharge into the Baltic sea above 61°N. Two of the largest rivers do however discharge below 61°N and the measurement site lies in the northernmost one of these, Dalälven (Dal River). The river originates in the west of Sweden in the mountains, and flows eastward having its outflow at 60°N.

The current velocity was measured in a channel by the city of Söderfors, located approximately 20 km upstream of the river's outlet in the sea. The chosen channel is 1 km long and it discharges into a lake. The cross section of the channel varies from a rectangular shape with a depth of ten meters and width of 30–60 m, to a parabolic shape 6 m deep and 100 m wide close to the lake. There are three bridges along the channel and the bridge furthest downstream was chosen as the measurement site, see Fig. 1(b).

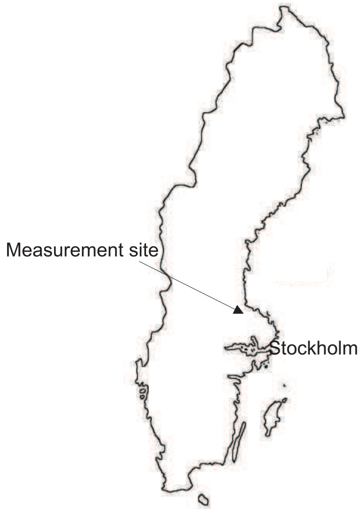

(a) Outline map of Sweden.

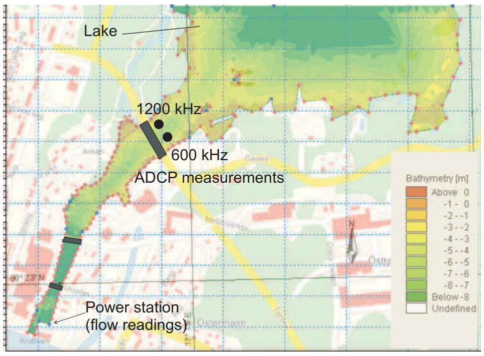

(b) Map of site.

Figure 1: Maps over the measurement site. In (b) the interpolated depths and the location for the deployment of the ADCPs are shown.

2.1 Data

To measure the velocities two ADCPs from RD Instruments, one 1200 kHz and one 600 kHz, were deployed for one month in the channel 800 m downstream of a hydropower station. During the measurement with the 1200 kHz ADCP external forces interrupted the data series at two occasions, resulting in three series of data. The measurement series for the 600 kHz ADCP was good for a period of 24 days. Measurement parameters are presented in Table 1. The ADCP uses an average of 50 pings to make one ensemble. Since the ensemble interval was 6 minutes, ten measurement readings were received per hour. Due to the built-in pressure sensor, total depth is also measured at 6 minute interval. The time-varying total depth deviation from the mean depth is the measured water level, denoted η_A. The 600 kHz instrument is meant to operate at depths greater than 20 m. At this occasion the instrument was deployed at a very shallow depth, resulting in large error velocity, sometimes exceeding 200 mm/s. The velocity data from this instru-

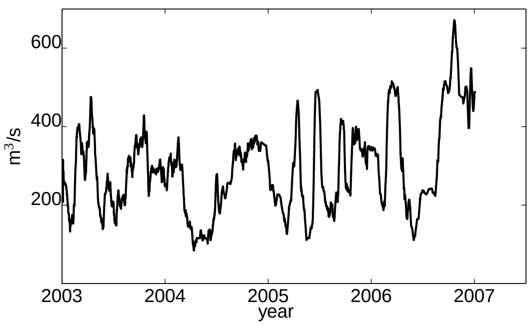

Figure 2: Weekly averaged flow in the channel by Söderfors 2003 - 2007.

Table 1: ADCP measurement parameters.

Frequency	1200 kHz	600 kHz
Ensemble interval	6 min	6 min
Pings/ensemble	50	50
Bin size	0.25 m	0.5 m
Measured depth range	4.5 m	2.5 m
ADCP depth	6.5–7 m	5.5–6 m
Duration of deployment	33 days	29 days
Standard deviation	96 mm/s	119 mm/s

ment has thus been omitted, but the water level readings were used to compare with the 1200 kHz ADCP, Fig 3.

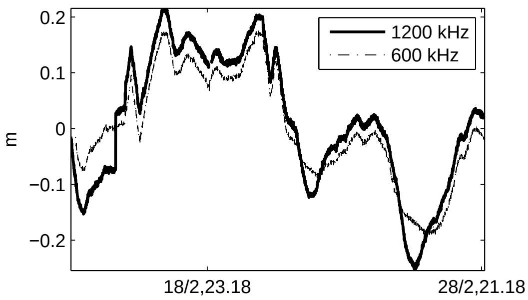

Figure 3: Water level measured by the two ADCPs.

The data from the ADCP was compared with flow and water level readings. The hourly averaged flow data was provided by Vattenfall AB; the owners of the hydropower station upstream of the sampling location. Hourly water level measured in the downstream lake were received from Fortum AB and is denoted η_L. The data was taken from a water gauge station in the downstream lake (not on the map), but there was no information on the accuracy of the data.

The yearly flow variation, seen in Fig. 2, shows a mean flow of 300 m^3/s and a maximum flow that exceeds 600 m^3/s.

3 Numerical modeling

To model the river, a 2D numerical program, Mike21, from the DHI Group in Sweden was used. The program is capable of modeling various processes, e.g. sediment transport, but the simulations were performed including only basic properties such as bottom stress. The governing equations are the well known depth averaged shallow water model. The main equations are well described in [8] and are therefore omitted from this work. The equations used to describe the conditions at the site are presented below.

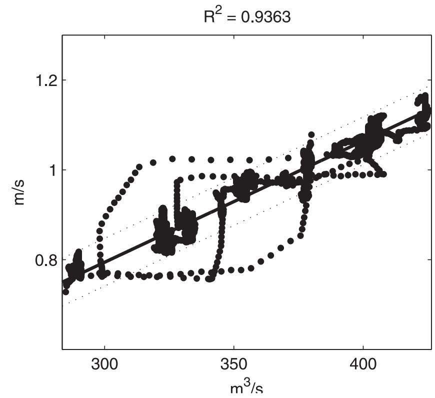

Figure 4: Regression plot between hour averaged ADCP current speed and flow.

3.1 Theory

In Mike21 Flow model FM [8], bottom friction is assumed to vary quadratically with the velocity above the bottom according to

$$\vec{\tau}_b = \rho c_f \vec{u_M} \left| \vec{u_M} \right| .$$

The drag coefficient, c_f, can be calculated using the Manning number, M as

$$c_f = \frac{g}{\left(Mh^{1/6}\right)^2} . \quad (1)$$

h is the total depth which is the sum of the still water depth, d and water level deviation from this, η_M. The Manning number represents the bottom surface roughness and is the resistance to flow in channels. It depends on factors such as the type and size of the material of the channel, and the shape of the channel [9].

Lateral turbulence is modeled using a sub–grid scale horizontal eddy viscosity concept as proposed in [10]. The horizontal eddy viscosity, ν_t, is related to a characteristic length scale (grid length scale), l, according to

$$\nu_t = c_s^2 l^2 \sqrt{2S_{ij}S_{ji}} , \quad (2)$$

where c_s is the Smagorinsky coefficient and S_{ij} is the deformation rate given by

$$S_{ij} = \frac{1}{2}\left(\frac{\partial u_i}{\partial x_j} + \frac{\partial u_j}{\partial x_i}\right)(i, j = 1, 2) .$$

3.2 Model setup

The studied area was modeled with a flexible mesh system, allowing variable sized mesh where desired. The meshed domain includes 2518 nodes and 4652 elements.

Table 2: Mike 21 parameters.

Simulation	Validation
Time period	090204 – 090228
Time step	360 s
Nr of time steps	2500
South boundary	Q (Fig 6(a))
North boundary	η_L (Fig 6(c))
Manning number	32 $m^{1/3}$ s^{-1}
c_s	0.28

Bathymetry data, Fig. 1(b), was received from measurements, maps and drawings for the area. Due to the bathymetry data being rather scarce, it is considered one of the greatest sources of errors for the simulation.

As an input to the model both the Manning number and a value for the Smagorinsky formulation is required. Since it is a dredged channel and the surrounding area is of sand and gravel, the Manning number was set to 32 $m^{1/3}s^{-1}$ which corresponds to a rather smooth surface [9, 11], and c_s in Eq. 2 was set to 0.28.

The simulations were executed as shown in Table 2 to validate the numerical model. The two open boundaries were the power station (south) and the lake (north). Flow readings for February were used at the first boundary and water level for February at the second.

Data from the numerical model was extracted at the location of the two ADCPs, which were deployed in between and slightly downstream two pillars.

Further simulations were done to estimate current speed for different flow rates with and without including turbines. The same parameters for n and c_s were used.

3.3 Including turbines

In this study the interest is in estimating how the water level and velocity along the channel are affected by energy extraction. Turbines can be added in the model and are then assumed to induce a drag force, F_t, on the flow. This is calculated according to

$$F_t = \frac{1}{2}\rho c_d A_e V^2 \ .$$

A_e is the effective area of the turbine on which V acts. Note that V is the velocity experienced by the turbine, and not the undisturbed velocity, U_M. The drag coefficient, c_d, increases the blockage effect on the flow, which in turn decreases the velocity, V. The power extraction by each turbine can be calculated using

$$P = F_t V. \qquad (3)$$

As the value of c_d increases, the extracted power increases, but this effect is diminished at high values of c_d, since the velocity goes toward zero (Fig. 7). However, at these values the devices could be regarded as pillars since no flow is passing through, and it is thus not realistic to apply very high values of c_d.

Turbines were modeled as a retarding force on the flow in e.g. [12]. The one-dimensional model indicated the velocity in the channel would decrease in total when extracting energy. In this study, the numerical model is two-dimensional and effects on the surrounding flow field can be expected to be somewhat different, since it is possible to account for wake effects and a velocity increase around the turbines.

A set of 10 turbines were included in the model and distributed pair-wise along the channel (Fig. 5). The structure of the farm has not been optimized to give maximum power output, but to simulate effects on the surrounding flow. The distance was approximately ten diameters in between each row.

Each turbine had a quadratic cross section area, A_e, see Table 3. The effects on the water level and velocity in the channel for the turbine setup could be calculated for several flow rates and c_d-values.

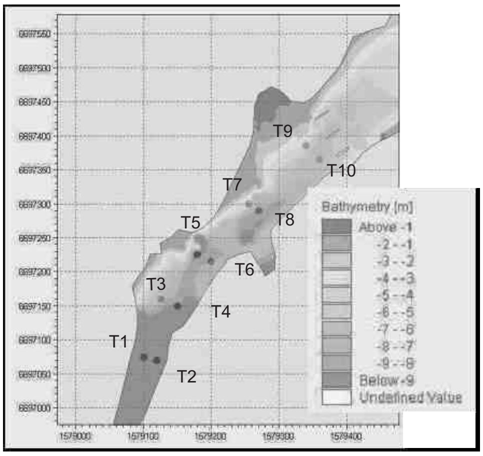

Figure 5: Turbine configuration.

4 Results and discussion

There is a good correlation between measured hourly averaged ADCP data and flow readings seen from the correlation coefficient, R^2, of 0.94 as seen in Fig. 4. This could be expected due to the proximity of the measurement site to the power station. The correlation value indicates the flow data is good to use to describe the current speed in the channel.

The level data for the lake (η_L) was received separately from the flow values, and no accuracy is available. It can be seen in Fig. 6(c) that η_A and η_L vary independently from each other, which is a result of spatial variations of the lake water level.

4.1 Validation of the numerical model

The above mentioned results indicate that the velocity in the channel depends mostly on the flow. Thus, the received flow readings were applied at the power station boundary. η_L was applied at the second boundary. The simulation was performed to compare with measured data, and due to the interruption during measurements, the simulation was only run for existing sets of data. This explains the gap in the Mike21 series in Fig. 6.

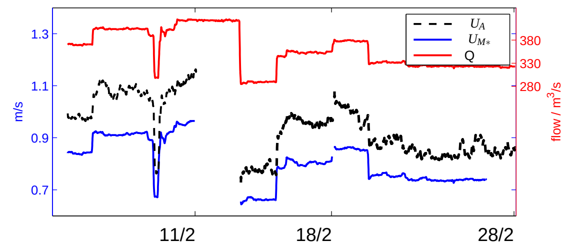

(a) Current speed.

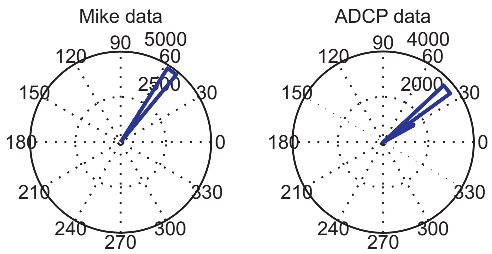

(b) Rose plot.

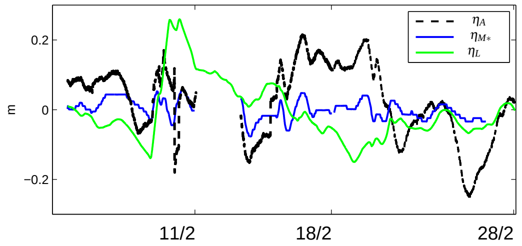

(c) Water level.

Figure 6: Mike data extracted from the measurement location by the bridge and ADCP data from the 1200 kHz instrument. (a) Current speed at the bridge (left axis, U_{M*} and U_A) compared with flow at power station, Q. (b) Rose plot between measured and modeled current direction data (c) Water level at the bridge (η_L and η_A) compared with water level at the lake boundary.

In the same figure it is seen that U_{M*} follows U_A closely, but the magnitude of the simulated current speed is slightly lower. This is probably due to bathymetry errors. As mentioned previously, there were some difficulties in re-creating the bathymetry due to scarce data. The bathymetry could be improved by more measurements. At the shallow depths as in the present channel, small changes in the bathymetry greatly alter the flow field.

The rose plot in Fig. 6 shows there is a slight deviation in the modeled current direction compared with the measured one. The ADCP was located downstream a few bridge pillars where the flow is turbulent. Therefore, depending on the cross-channel position, the flow direction can vary. The deviation can be a result of that the data from the simulation was extracted from a location slightly different than from the measured one.

Fig. 6(c) shows the simulated (η_{M*}) and measured (η_A) water level deviations from mean. Although η_{M*} at times shows the same variation as η_A, the model is not able to simulate the magnitude of the water level. The maximum variation ($\max(\eta) - \min(\eta)$) of η_A was 0.47 m while for η_{M*} the maximum variation was 0.13 m.

The model assesses the current speed reasonably well, but not the water level deviations. Using more accurate bathymetry data and including other parameters such as wind data over the lake could have improved these results, but no such data was available.

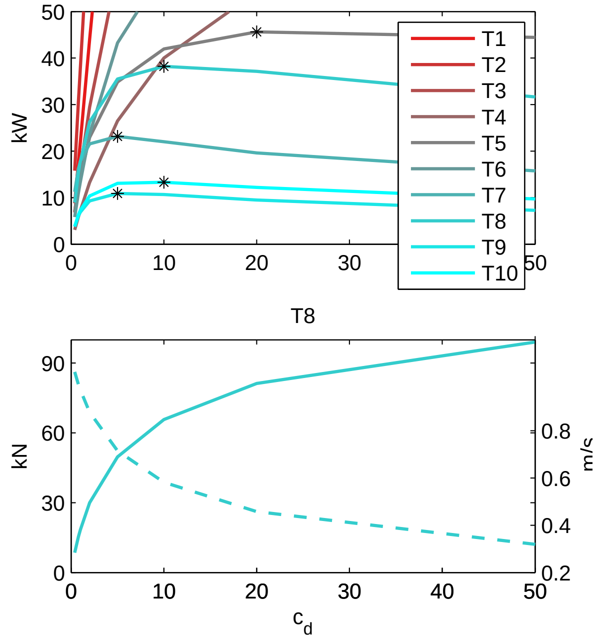

Figure 7: Top: Effects of c_d on power output modeled in Mike21 at a flow of 500 m^3/s. Maximum power for each turbine is denoted by *. Bottom: Force and velocity at turbine T8 with increasing c_d.

4.2 Turbine influence

The power output from each turbine was calculated for different c_d- and flow values using Eq. 3. In Table 3, the power output for three flow rates, 300 m^3/s (mean), 500 m^3/s and 700 m^3/s (maximum), is presented, showing the total power output is more than 10 times higher in the case for maximum flow as compared to the mean flow.

The power is proportional to the force of the turbine, which in turn depends on Q_t^2 (through the turbine) and c_d. Maintaining a constant flow in the channel, an increased c_d-value will decrease the flow through the turbine, a result of an enhanced flow at the sides of the turbine. At a certain c_d, the power output starts decreasing. Maximum power for each turbine in a flow of 500 m^3/s is plotted in Fig. 7. Comparing this plot with simple calculation using $P = \frac{1}{2}\rho A_e U^3$ shows that for a velocity of 1 m/s and a cross sectional area of 100 m^2, as is the case for turbine T1, the maximum kinetic energy is 50 kW. For turbine T1 and T2 this value is reached already at a c_d-value in between 1 and 2. It is thus not recommended to apply a c_d-value above 1 for realistic simulations.

In [12] the model was forced by a varying water level, and increased turbine drag resulted in a decreased velocity in the whole channel. Here, the driving force is a

Table 3: Power [kW] for three different flow rates. c_d-value is 0.8.

Turbine	T1+T2	T3+T4	T5+T6	T7+T8	T9+T10	Total
Cross section m^2	100	49	49	49	25	–
Flow 300 m^3/s	11	4.6	5.6	7.6	3.1	32 kW
Flow 500 m^3/s	48	19	23	32	12	135 kW
Flow 700 m^3/s	123	48	60	81	32	344 kW

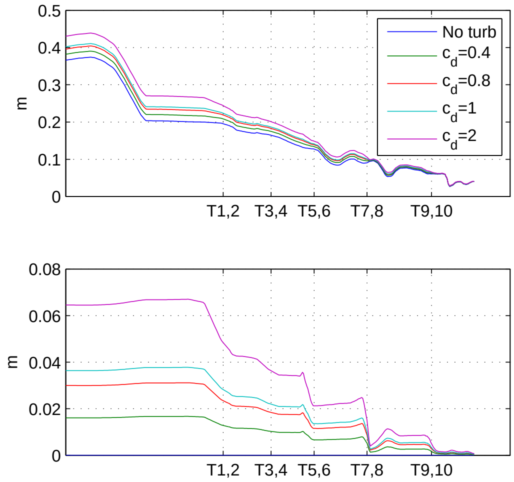

Figure 8: Effects of turbines on the water level along the channel for different c_d– values and a flow is 500 m^3/s. Top: Increase from the value at the lake. Bottom: Change in water level calculated as the difference from the case of no turbines.

constant flow, and increasing the turbine drag leads to a higher water level upstream. For continuity to be valid, the same flow must pass through all sections in channel, leading to an enhanced pressure force. This is the probable reason for the high power values achieved when increasing the drag force.

Modeling of turbine effects was performed both with and without turbines included; hence the difference in water level could be extracted for different c_d-values. The effects of this particular turbine configuration on surrounding water level are shown in Fig. 8 for flow rate of 500 m^3/s. For a case with no flow, the water level is zero everywhere. At a flow rate of 500 m^3/s and without any turbines, the water level at the power station is 36 cm higher than at the lake boundary. When including 10 turbines the water level at the power station is increased by an additional 1.6 cm using a c_d of 0.4 (75 kW) and 3 cm for a c_d of 0.8 (135 kW). This corresponds to a 5.5% and a 8.2% increase of the water level respectively, compared to the case without any turbines (Fig. 8). Note, however, that this result regards a constant water level at the downstream boundary.

In Fig. 9 the velocity field around all turbines is shown. The kinetic energy is proportional to the cube of the velocity, and the largest extraction rate can be found at the location of strongest currents. In Table 3 the presented values are per turbine, indicating T1 and T2 extracts most power. However, power per cross sectional area is highest for T7 and T8, which is coincident with

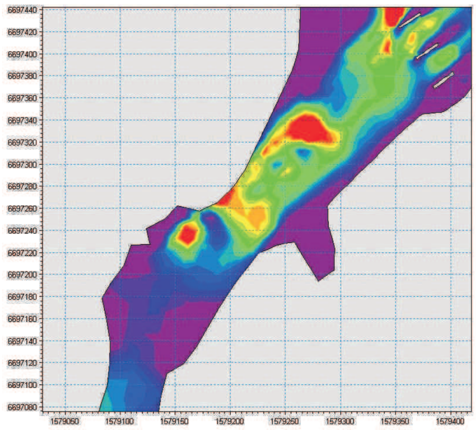

(a) No turbines.

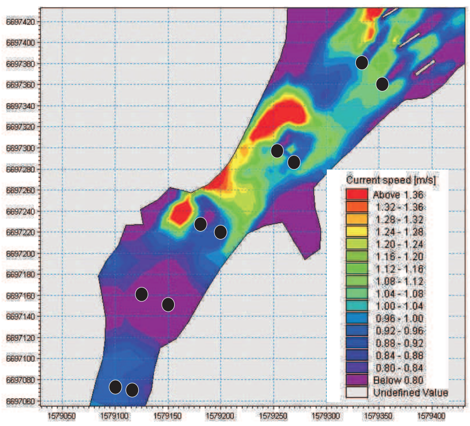

(b) 10 turbines.

Figure 9: Velocity field in the channel for the case of 10 turbines, c_d = 10.

where strongest currents can be found. The flow field around the turbines is modified locally, with enhanced current speed around the turbines, and decreased flow speed through the turbine and a few diameters downstream.

The modeled turbines have not been limited to a maximum power extraction, which is a questionable assumption. However, this report was made to investigate how the hydrography is altered when extracting kinetic energy, and not to study the theoretical potential of the channel. The results showed that power extraction and effects on the upstream water level is highly dependent on the chosen c_d-value.

It should be noted that for the parameters used in the simulation, the model was not able to correctly assess the water level deviation at the measurement site downstream the bridge. When simulating the turbine influence on the hydrography of the channel, the whole channel was considered, not only a single point. For this the model has not been validated. However, we are regarding an increase of water level due to energy extraction, and not the absolute value of the water level, and for this the results are still valid.

5 Conclusion

Measurements of current speed, current direction and water level have been compared with 2D-simulations done with the program Mike21. The simulation program was able to assess the current speed variations, but the modeled magnitude was slightly low, which is thought to be a result of bathymetry errors. The program could not assess the water level deviations well. This could be improved by adding wind data to the model, but no such data was available.

Variation of the hydrography due to turbines was studied. The set of turbines were chosen to experiment how the upstream water level is affected input flow and turbine drag is varied, and not to optimize energy extraction or to calculate the potential of the site. It showed that extracting 75 kW would increase the water level at the power station from the level without any turbines at the same location with 5.5%, and 135 kW would lead to an 8.8% increase, using the specified level at the downstream lake. Choosing the appropriate c_d-value for each turbine is of major importance since the effects on the hydrography is large.

Acknowledgments

The numerical program Mike21 was used with permission from Stefan Ahlman at the DHI Group in Sweden (www.dhi.se). The flow data was provided by Vattenfall AB (www.vattenfall.se) and water level readings are from FORTUM AB (www.fortum.se). This work was financed by Ångpanneföreningen's Foundation for Research and Development, Östkraft's Environmental Fund and Vattenfall AB. I would also like to thank my colleagues at The Swedish Centre for Renewable Electric Energy Conversion for helping out with the measurements and for their valuable comments on this article, and to Antoine Baudoin for his initiation of the grid.

References

[1] Vindkraftsstatistik 2007. The Swedish Energy Agency, ES 2008:02, publikationsservice@energimyndigheten.se, 2007.

[2] M. J. Khan, M. T. Iqbal, and J. E. Quaicoe. River current energy conversion system: Progress, prospects and challenges. *Renewable & Sustainable Energy Reviews*, 12:2177–2193, 2008.

[3] L. S. Blunden and A. S. Bahaj. Initial evaluation of tidal stream energy resources at Portland Bill, UK. *Renewable Energy*, 31(2):121–132, February 2006.

[4] L. S. Blunden and A. S. Bahaj. Effects of tidal energy extraction at Portland Bill, southern UK, predicted from a numerical model. In *Proceedings of the 7th European wave and tidal energy conference, EWTEC07, Porto, Portugal*, pages 1–10, September 2007.

[5] G. Sutherland, M. Foreman, and C. Garrett. Tidal current energy assessment for Johnstone Strait, Vancouver Island. *Proc. IMechE Part A: Journal of Power and Energy*, 221:147–157, 2007.

[6] J. V. Norris and E. Droniou. Update on EMEC activities, resource description, and characterisation of wave-induced velocities in a tidal flow. In *Proceedings of the 7th European wave and tidal energy conference, EWTEC07, Porto, Portugal*, September 2007.

[7] R. Carballo, G. Iglesias, and A. Castro. Numerical model evaluation of tidal stream energy resources in the Ría de Muros (NW Spain). *Renewable Energy*, 34(6):1517–1524, 2009.

[8] Mike 21 and Mike 3 flow model FM, hydrodynamic and transport module. scientific documentation, 2008. DHI.

[9] G. J. Arcement and V. R. Schneider. Guide on selecting Manning's roughness coefficients for natural channels and flood plains. Water-supply paper WSP2339, Unites States Geological Survey, 1984.

[10] J. Smagorinsky. General circulation experiments with the primitive equations. *Monthly Weather Review*, 91(3):99–164, March 1963.

[11] Pierre Y. Julien. *River mechanics*. Cambridge University Press, Cambridge, 2002.

[12] I. G. Bryden, S. J. Couch, A. Owen, and G. Melville. Tidal current resource assessment. *Proc. IMechE Part A: Journal of Power and Energy*, 221:125–135, 2007.